

Formation and motion of horse collar aurora events

G.E. Bower¹, S.E. Milan^{1,2}, L.J. Paxton³, E. Spanswick⁴ and M.R. Hairston⁵

¹ School of Physics and Astronomy, University of Leicester, UK

² Birkeland Centre for Space Science, Bergen, Norway

³ Johns Hopkins University Applied Physics Laboratory, USA

⁴ Department of Physics and Astronomy, University of Calgary, Calgary, Alberta, Canada

⁵ Space Science Center, University of Texas at Dallas, Richardson, TX, US

Key Points:

- Horse collar aurora evolution is dependant on changes in the interplanetary magnetic field orientation.
- Horse collar aurora arcs move dawnward in the northern hemisphere if the interplanetary magnetic field becomes negative IMF B_y dominated.
- Transpolar arcs and horse collar aurora can occur simultaneously.

Abstract

The polar cap can become teardrop shaped through the poleward expansion of the dusk and dawn sectors of the auroral oval, to form what is called horse collar aurora (HCA). The formation of HCA has been linked to dual-lobe reconnection (DLR) where magnetic flux is closed at the dayside magnetopause. A prolonged period of northward IMF is required for the formation of HCA. HCA have previously been identified in UV images captured by the Special Sensor Ultraviolet Spectrographic Imager (SSUSI) instrument on-board the Defense Meteorological Satellite Program (DMSP) spacecraft F16, F17 and F18. Events that have concurrent 630.0 nm all-sky camera (ASC) data from the Redline Geospace Observatory (REGO) Resolute Bay site are now studied in more detail, making use of the higher cadence of the ASC images compared to DMSP/SSUSI. 11 HCA events are studied and classified based on the IMF conditions at the end of the event. Five of the events were found to end via a southward turning of the IMF, two end with positive B_y dominated IMF and four with negative B_y dominance. Under positive (negative) B_y the arcs move duskward (dawnward) in the northern hemisphere with the opposite true in the southern hemisphere. Under a southward turning the arcs move equatorward. One event is of particular interest as it occurred while there was a transpolar arc (TPA) also present. Understanding the evolution of HCA will allow DLR to be studied in more detail.

Plain Language Summary

Horse collar auroras (HCA) form when the auroras move to high latitudes at dawn and dusk resulting in a teardrop-shaped polar cap. When the interplanetary magnetic field (IMF) embedded in the solar wind is directed almost exactly northwards a process called dual-lobe reconnection can occur which closes open magnetic flux on the dayside of the magnetosphere and has been proposed to be linked to the formation of HCA. We investigate 11 events in further detail that have concurrent data from Defense Meteorological Satellite Program and the 630.0 nm all-sky camera from the Redline Geospace Observatory. The events are separated based on the IMF conditions at the end of the event which appears to determine their subsequent evolution. The IMF turns southward at the end of 5 events, for the other 6 the IMF becomes dominated by a dawnward (2 events) or a duskward (4 events) component. One event is of special interest as the HCA occurs alongside a transpolar arc, where a single band of aurora is seen poleward of the main auroral oval. Studying the evolution of HCA and the solar wind conditions under which they evolve allows us to gain new insights into the conditions necessary for DLR.

1 Introduction

Hones et al. [1989] first defined horse collar aurora (HCA) in 1989 based on Dynamics Explorer 1 auroral imager observations and derived their name due to the shape of the emitting area. HCA consist of bars of aurora in the morning and evening sectors framing a polar slot. Equatorward of the bars are 'webs', which are regions of soft particle precipitation which contain weak (sometimes subvisual) aurora. HCA have been confirmed to occur when the interplanetary magnetic field (IMF) is northward, particularly at times when the B_y component is small [Hones et al., 1989, Meng, 1981, Murphree et al., 1982, Zhu et al., 1997, Bower et al., 2022]

In early observations, Hones et al. [1989] reported a possible relationship between the location of the HCA polar slot and the IMF B_y component. They observed a HCA on 9th May 1983 that formed around 08:23 UT and persisted until after 10:35 UT. During the HCA the IMF B_z component was consistently around +5 nT however the IMF B_y component was variable, being predominately negative before a sharp change at 09:20 UT after which it remained positive. Tracking of the polar slot between images over this time showed a dawnward motion of the HCA configuration after the B_y change. In the present study we investigate in more detail how changes in the orientation of the IMF affect pre-existing HCA, with the aim of further understanding their formation and subsequent disappearance.

A thickening or tilting of the central plasma sheet have been suggested as possible formation models of HCA [Meng, 1981, Makita et al., 1991]. Meng [1981] suggested that a thickening of the central plasma sheet at both dawn and dusk could lead to a poleward expansion of the auroral oval at both sides, with this expansion of the auroral oval leading to the HCA configuration. MHD simulations by Tanaka et al. [2017] also show a significant thickening of the plasmas sheet on both sides forming a HCA configuration produced by a group of small-scale Sun-aligned arcs in the field-aligned currents (FACs) distribution [Hosokawa et al., 2020].

Recently Milan et al. [2020] proposed a new model of HCA formation based on dual-lobe reconnection (DLR). DLR occurs under northward IMF when the same magnetic field line reconnects in both lobes of the Earth's magnetosphere such that previously open field lines become closed. Milan et al. [2020] suggest that this newly closed flux is redistributed to dawn and dusk causing the open-closed field line boundary (OCB) to move poleward at dawn and dusk creating the HCA configuration and the distorted polar slot. There are also strong sunward flows across the dayside polar cap boundary as flux is converted from an open to closed topology. During this the main auroral oval remains relatively unchanged. Figure 3 of Milan et al. [2020] shows this schematically.

Milan et al. [2020] also suggested the anticipated response of the HCA configuration to changes in IMF orientation. Following a southward turning of the IMF, low-latitude reconnection leads to the creation of new open flux at the dayside of the polar cap. This newly open flux will be redistributed via a twin-cell convection pattern as the main auroral oval expands to lower latitudes, shown schematically in figure 7b of Milan et al. [2020]. This convection pattern is suggested to effect the HCA regions with them being pushed towards the nightside. A non-zero IMF B_y component will lead to the convection pattern being distorted to have a dusk-dawn asymmetry [Goudarzi et al., 2008]. The HCA arcs should be entrained within the flows such that for positive B_y the newly open flux is distributed asymmetrically at dawn and lead to a general duskward motion of the closed high latitude flux of the HCA in the northern hemisphere, shown schematically in figure 7c of Milan et al. [2020].

Milan et al. [2020] also suggested that the HCA configuration will evolve if the IMF stays northward but develops a non-zero B_y component, shown schematically in figure 7d of Milan et al. [2020]. In this case single-lobe reconnection (SLR) occurs in which magnetic field lines in the lobes of the magnetosphere reconnect with the IMF independently in both hemispheres. This leads to no changes in the amount of open flux within the polar cap but it is redistributed. In the case of positive B_y in the northern hemisphere open flux is siphoned from the pre-existing polar cap to create a new region of open flux at dawn [Milan et al., 2005]. This motion is suggested to cause the closed flux of the HCA to move together and duskward in this scenario. It is also possible for a smaller second reverse cell to be present [Imber et al., 2006, Milan et al., 2020] that could then create a smaller open region at dusk. The motion of the HCA arcs in the northern and southern hemisphere can be independent of one-another as SLR can occur at different rates in both hemispheres.

All-sky cameras (ASC) have commonly been used to look at auroral arcs. Hosokawa et al. [2020] reported on a HCA event which occurred on 6th January 2013 where the ASC at Resolute Bay, Canada was able to observe the dawnside web of a HCA. At the same time space-based observations were available from SSUSI (Special Sensor Ultraviolet Spectrographic Imager) instrument on board a Defense Meteorological Satellite Program (DMSP) satellite showing the whole HCA configuration. The ASC showed the web to be formed of a number of small-scale sun aligned arcs. Both types of auroral observation have their strengths and weaknesses. SSUSI has near-global coverage but poor temporal resolution, such that the evolution of auroral features is difficult to determine. On the other hand, ASC have a limited viewing area, but excellent time resolution. In this study we combine SSUSI with ASC to learn more about how HCA wax and wane.

In this paper we study the evolution of the 11 HCA events reported by Bower et al. [2022] in SSUSI observations that have concurrent Resolute Bay ASC data. The instruments used are described in section 2. Section 3 focuses on the observations of each event individually. The observations are discussed in section 4 in relation to the Milan et al. [2020] model which has been adapted to include the presence of a transpolar arc in explanation of one of the HCA events discussed. Finally section 5 concludes.

2 Instrumentation

We make use of two instruments on-board the Defense Meteorological Satellite Program (DMSP) satellites, the Special Sensor Ultraviolet Spectrographic Imager (SSUSI) and the Ion Drift Meter (IDM). DMSP is a series of sun-synchronous orbiting spacecraft with an altitude of 833 km (nominal) and an orbit period of 101.6 min [Paxton et al., 1992]. The particular spacecraft used here are F16, F17 and F18.

SSUSI provides scans of the polar regions of the Earth. Each scan is a swath of the region built up over ~ 20 minutes by scanning transverse to the orbit; each hemisphere is scanned approximately every 50 min. SSUSI operates at multiple wavelengths though we have only used the LBHs data as this is the clearest [Paxton et al., 1992, 1993, 2017].

IDM is a sensor that is one of the four parts that make up the thermal plasma array detector SSIES (the special sensor for ions, electrons, and scintillation). It provides horizontal and vertical ion drift velocities at a rate of 6 samples per second with a resolution of 12 m s^{-1} . The IDM measures the ion drift velocity perpendicular to the spacecraft’s velocity by measuring the angle of arrival of the ions. From this angle of arrival the perpendicular ion drift velocity is inferred since with respect to DMSP’s velocity the thermal velocity of ions is negligible [Rich and Hairston, 1994].

Alongside the DMSP instruments we make use of three all-sky cameras (ASC) from the Red-line Geospace Observatory (REGO) system. The REGO is a system of auroral all-sky imagers designed and operated by the Auroral Imaging Group (AIG) which is part of the Canadian Space Agency’s Geospace Observatory (GO) Canada initiative [Calgary, 2022]. The imagers operate at 630.0 nm, which is red-line optical emission, and have high sensitivity and temporal resolution, operating at a 3 s cadence with 2 s exposure time, and as such are able to detect faint polar cap aurora [Liang et al., 2016]. The three ASC used are Resolute Bay (geographic latitude 74.7° , longitude 265.17°), Taloyoak (geographic latitude 69.54° , longitude 266.45°) and Rankin Inlet (geographic latitude 62.82° , longitude 267.89°). All-sky camera data is only available during

local winter and when the local solar zenith angle is greater than 102 (i.e., it is dark enough to see the aurora).

3 Observations

From the list of 642 HCA events found by Bower et al. [2022] there are 11 events that coincide with Resolute Bay all-sky camera (ASC) data, listed in Table 1. Two other high latitude ASC are also used when data is available, these are the Rankin Inlet camera and the Taloyoak camera. Whether this data is available for an event or not is indicated in Table 1.

Event number	Event date	Start time (UT)	End time (UT)	All-sky Camera data	IMF data	IMF ending event
1	2014-11-10	22:07	21:15	Resu, Rank, Talo	ACE	Dominant Negative B_y
2	2014-11-28	08:02	12:15	Resu, Talo	OMNI	Southward turning
3	2014-11-30	09:20	16:24	Resu, Talo	OMNI	Dominant Negative B_y
4	2014-12-13	09:51	13:42	Resu, Talo	ACE	Southward Turing
5	2014-12-31	16:46	04:26	Resu, Talo	OMNI	Dominant Negative B_y
6	2015-10-24	08:26	13:39	Resu	OMNI	Southward Turing
7	2016-01-02	21:20	04:48	Resu	ACE	Southward Turing
8	2016-01-04	09:24	12:20	Resu	ACE	Southward Turing
9	2016-01-05	12:59	19:20	Resu, Rank	ACE	Dominant Positive B_y
10	2016-02-03	09:51	18:49	Resu, Rank	OMNI	Dominant Positive B_y
11	2016-12-12	11:07	19:39	Resu, Rank, Talo	OMNI	Dominant Negative B_y

Table 1: Table of HCA Events. The ASC used with data available for the events are indicated in the fifth column. The final column show the IMF condition at the end of the event which the events have been categorized with.

Due to large gaps in the OMNI data, magnetic field data from ACE is used for some events. In order to propagate this data to the magnetopause the position of the magnetopause is calculated using an assumed solar wind density of 3 cm^{-3} and the measured solar wind velocity along with the location of the ACE spacecraft. This density is used as there is no density data from ACE at these times and is an average solar wind density.

Out of the 11 events, 5 were found to end with a southward turning of the IMF. The other 6 events end with either positive (2 events) or negative (4 events) B_y dominated IMF. Event

1 is a special case where a TPA is present before the HCA forms. The events are described in detail below; they have been grouped based on the IMF condition at the end of the event.

3.1 Southward turning

We now present event 2 and discuss events 4, 6, 7, and 8 which are periods of HCA which end with a southward turning of the IMF.

Figure 1 shows key times during event 2 on 28th November 2014. The top two panels show ASC data keograms across the north-south line (i) Resolute Bay and (ii) Taloyoak. The IMF data is shown in the next panel (iii), the B_z component is indicated by the black line, the B_y component by the red line and the B_x component by the blue line. The bottom panels show the different times vertically in each column with the spacecraft and hemisphere of the DMSP observations given in the first row along with them time in UT. The first row of the columns shows the DMSP/IDM flows with an inset showing the IMF clock angle at the time of the SSUSI image. The second row is the LBHs SSUSI image with the field of view of the ASC overlaid. The third row is the SSUSI image centred on the Taloyoak ASC station with the resolute bay and Taloyoak ASC images projected on top. The final rows are the ASC images, first from Resolute Bay and secondly from Taloyoak.

Event 2 began around 08:02 UT (Figure 1a) on 28th November 2014 when the IMF changed from a negative B_y dominated IMF to a more northward IMF, the clock angle briefly passed through -9.8° before settling between -40 and -30° . The HCA pattern could be seen forming in the northern hemisphere around this time and was also visible in the next southern hemisphere SSUSI image (Figure 1b). Sunward flows were seen across the centre of the polar cap during the event (Figure 1), with antisunward flows to either side, consistent with the DLR formation scenario outlined by Milan et al. [2020]. During this event there was a period of negative B_y and the dawnside arc in the northern hemisphere appeared the brightest of the two arcs (Figure 1c).

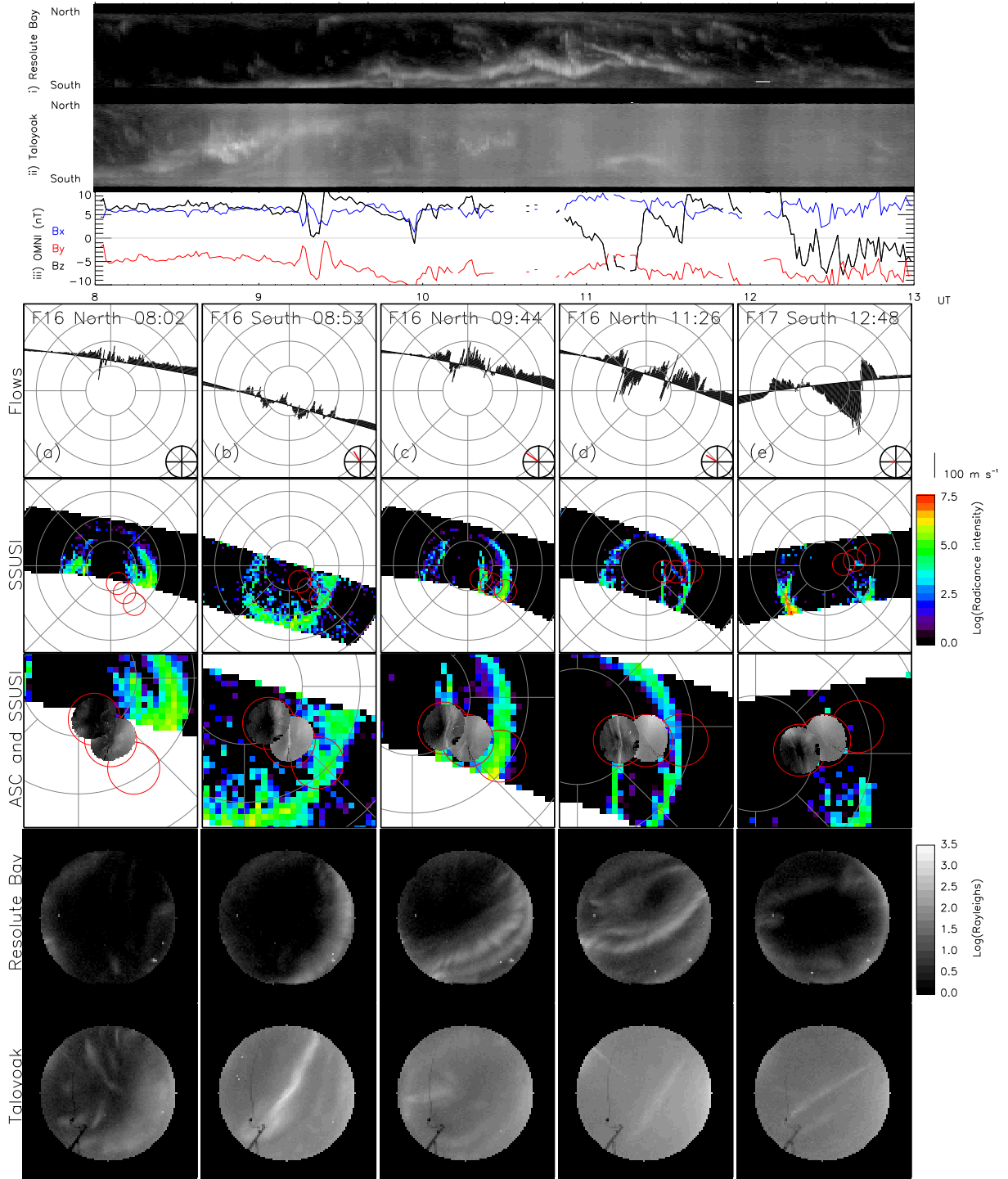


Figure 1: Event 2 SSUSI and ASC images. The top panels show the keograms of the ASC and the relevant IMF data for the event. The first row of the columns shows the DMSP/IDM flows with an inset showing the IMF clock angle at the time of the SSUSI image. The second row is the LBHs SSUSI image on a log scale. The third row is the SSUSI image centred on the Taloyoak ASC station with the available ASC images projected on top. The final rows are the ASC images with north located at the top of each image plotted on a log scale. The UT given is the time of the ASC image and the most poleward point of the DMSP pass.

From the ASC and SSUSI row in Figure 1 it can be seen that ASCs show consistency with the SSUSI images. It is clearly seen that the ASC is observing the dawn HCA auroral arc due to the way they line up particularly in Figure 1d. The ASCs clearly showed the dawnside arc moved poleward, first seen by the Taloyoak camera and then by the Resolute Bay camera (Figure 1). The Resolute Bay ASC also showed the retreat of the arc back equatorward, coinciding with a brief southward turning of the IMF around 11:06 UT, before the longer turning of the IMF at 12:15 UT which ended the event. The southern hemisphere SSUSI image at 12:48 UT (Figure 1f) showed the retreat of the HCA arc back into the main auroral oval on both sides. The ASCs at that time showed that a similar retreat was happened in the northern hemisphere.

It is also important to note that there are multiple arcs seen in the HCA configuration not just the two main poleward arcs. This is particularly clear after around 10:15 UT when it can be seen that Resolute Bay and Taloyoak are observing different auroral arcs. The arc seen by Resolute Bay is believed to be the leading poleward edge arc, where the arc seen by Taloyoak is thought to be contained within the 'web' of the HCA.

In summary, this event shows the formation of HCA as observed by SSUSI under northward IMF during near-zero clock angle. The ASC observations show that the dawn HCA arc progresses polewards from the poleward edge of the dawn sector auroral oval, and then retreats equatorwards again once the IMF turns southwards.

Events 4, 6, 7 and 8 also show similar behaviour, each shows the formation of a HCA as observed by SSUSI during near-zero clock angle. During event 4 after formation of the HCA the clock angle settled around 40° . Clear sunward flows were seen across the polar slot of the HCA in the IDM data. The ASC viewed the dawnside arc of the HCA which moved poleward followed by other auroral arcs possibly making up the 'web' of the HCA. The event ended with a southward turning of the IMF and the arcs of the HCA are seen to move equatorward in both the SSUSI data and the ASC data.

The IMF has a slight B_y dominance at the start of event 6 but as this reduced and the clock angle then decreased to less than 40° the formation of the HCA becomes clearer. Sunward flows over the polar cap are again seen in the IDM data while the HCA configuration is present. The ASC data is only available for the start of the event and is hindered by cloud therefore no clear motion is seen; however the arcs do match the dawnside arc seen by SSUSI. The arcs remained relatively stationary and the presence of the sunward flow only ended once the IMF had turned southward. The following SSUSI images showed the arc in the southern hemisphere had moved equatorward.

For event 7 the ASC were observing the duskside arc toward the dayside initially and a poleward motion of the arc was seen while the IMF was near pure northward. The IDM data for this event were not very useful as they are usually towards the dayside or nightside edge of the oval thus not giving a clear indication of the HCA flows. At the end of this event the IMF B_z went southward with strong positive B_y . Following this change arcs were seen to move southward by the Resolute Bay ASC. The SSUSI images for the end of the event were very far towards the nightside and as such the arcs could not be seen.

The beginning of event 8 is hard to determine due to both a data gap in the SSUSI images and the Resolute Bay ASC not seeing any auroras. The IMF had a clock angle of $\sim 30^\circ$ at which time the oval was seen thickening at dawn and dusk by SSUSI. Following this the polar cap became smaller and aurora was seen in the Resolute Bay camera moving northward. The IMF briefly became dominated by negative B_y before it turned southward. After the southward turning the IMF was B_y positive and the arc was seen to move equatorward. Then the IMF changed from B_y positive to B_y negative and the dawnside arc seen by the ACS moved poleward before fading entirely when the IMF again turned southward.

3.2 Dominated Negative B_y

Here we present event 3 as well as discuss events 5 and 11, which are periods of HCA which end with the IMF being dominated by negative B_y . Event 1 is discussed separately.

Event 3 began around 9:20 UT on 30th November 2014. The HCA pattern was first seen around 9:20 UT (Figure 2a). This was after a period of northward IMF between 08:22 UT and 08:56 UT. The Resolute Bay camera also imaged aurora which moved poleward (Figure 2). A southward turning of the IMF at 9:38 UT halted the formation and the arcs moved anti-sunward.

When the IMF returned northward it was also B_y positive. In the northern hemisphere the dawn arc had moved towards a more central position and the dusk arc started to bend. The IMF became more purely northward around 13:22 UT although the OMNI data had short gaps around that time. The polar cap filled with aurora again and the flows were sunward.

Two new HCA arcs formed during the second period of northward IMF and the original arc appeared to be trapped in the middle. This is seen in the Resolute bay images as the new dawnside arc was seen from around 13:30 UT and moved poleward where it was clearly seen to align with the dawnside arc seen by SSUSI (Figure 2e). The IMF became B_y negative dominated, in the northern hemisphere the arcs were pushed downward and duskward in the

southern hemisphere. The IMF then turned southward and the arcs were no longer visible by 16:24 UT.

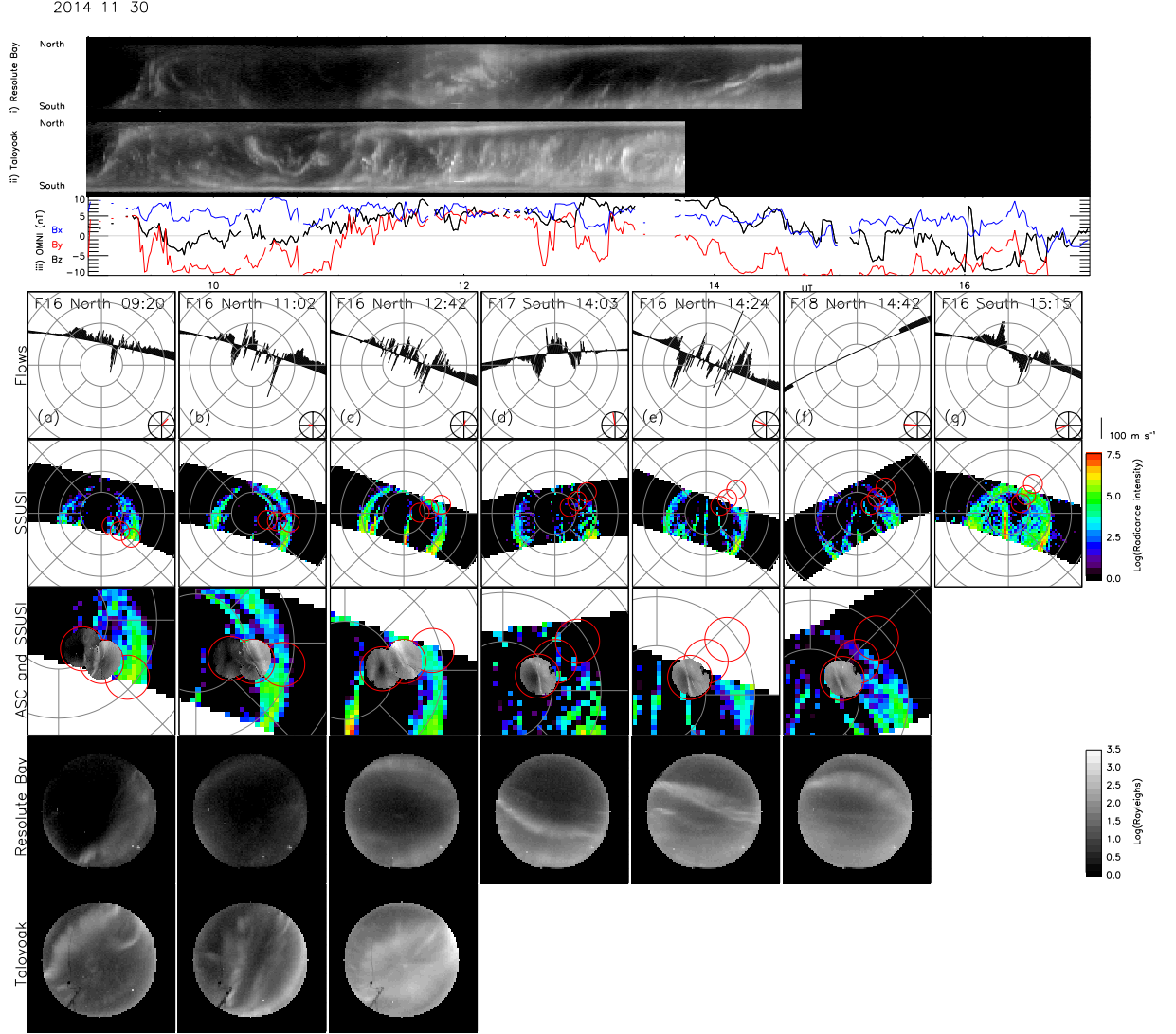


Figure 2: Event 3. Same format as Figure 1

In summary, SSUSI observed the formation of the HCA after a period of near-zero clock angle. During the event the ASC observed the dawn side arc moving poleward. After a period of variable B_y a second pair of HCA arcs formed with a single arc being left visible between them. After the IMF became B_y negative dominated the pair of HCA arcs both moved downward in the northern hemisphere and duskward in the southern hemisphere.

Events 5 and 11 also show similar behaviour. Event 5 started with sunward flows seen in the IDM data across the polar cap shortly after a period of pure northward IMF. The auroral oval was seen thickening at both side however a period of negative B_y dominated IMF appeared to halt the formation. Possibly, due to the B_y influence the arc at dusk in the southern hemisphere

then protruded further into the polar cap while the dawn arc in the northern did the same. The ASC were not ideally located being on the dayside and not imaging the HCA arc until the end of the event. The presence of the Moon also made the arcs less clear. The HCA pattern briefly faded before it emerged again when the clock angle was close to zero. The HCA pattern did not fully form in this event however SSUSI was able to see the dawnside arc in the northern hemisphere at the same time the ASC were viewing the duskside arc. The SSUSI images between 03:10 UT and 04:00 UT were not ideal as they only imaged the nightside thus it was not possible to see the arcs progression. By 04:26 UT the HCA pattern had gone and the dawn arc was merged back into the auroral oval. However the ASC saw the duskside arc progress poleward out of their field of view.

The formation of the HCA for event 11 was captured by the ASC as there were multiple gaps in the SSUSI data. When the clock angle became small a poleward motion of the dawnside arc was seen by both ASCs. There were also other smaller arcs in the Taloyoak images that also moved northward, these were likely in the web of the HCA. Small sunward flows over the polar cap were also seen at this time. Multiple arcs seen by the ASCs continued to move northward until a slight positive B_y dominance stopped the motion briefly; the arcs continued to move northward after. The sunward flows in this event were clearer in the southern hemisphere. The ASC data had gaps due to the time of day and the sun obscuring the view. After a period of variable IMF it finally remained B_y negative ending the near pure northward IMF. The HCA pattern was no longer visible in the northern hemisphere SSUSI image and instead a single dawnside arc was visible. By the following northern SSUSI image this arc had disappeared. A similar pattern was seen in the southern hemisphere: the remnant of the HCA pattern with a duskside arc in the following SSUSI image which had also gone by the following SSUSI image.

3.2.1 Event 1

At 10:03 UT on 11th November 2014 a clear HCA shape was visible in the SSUSI data (Figure 3k) thus suggesting that the actual start time of the event must be earlier than 10:03 UT. The IMF began to remain northward for a prolonged period from around 17:00 UT on the 10th November. Two TPAs were seen forming on opposite sides of the polar cap in the southern hemisphere at dusk around 18:28 UT and at dawn in the northern hemisphere 18:44 UT on the 10th November 2014 (Figure 3a and b). For at least an hour before the IMF was northward and the B_y component was negative around -6nT. The flows seen by DMSP were complicated with some sunward flows seen between 18:28 UT and 19:19 UT. At 20:09 UT and 20:26 UT the TPAs are not as clearly defined. The arc in the northern hemisphere was visible in the 21:01

293 UT image. During this period the IMF was quite variable with large B_y components.

2014 11 10

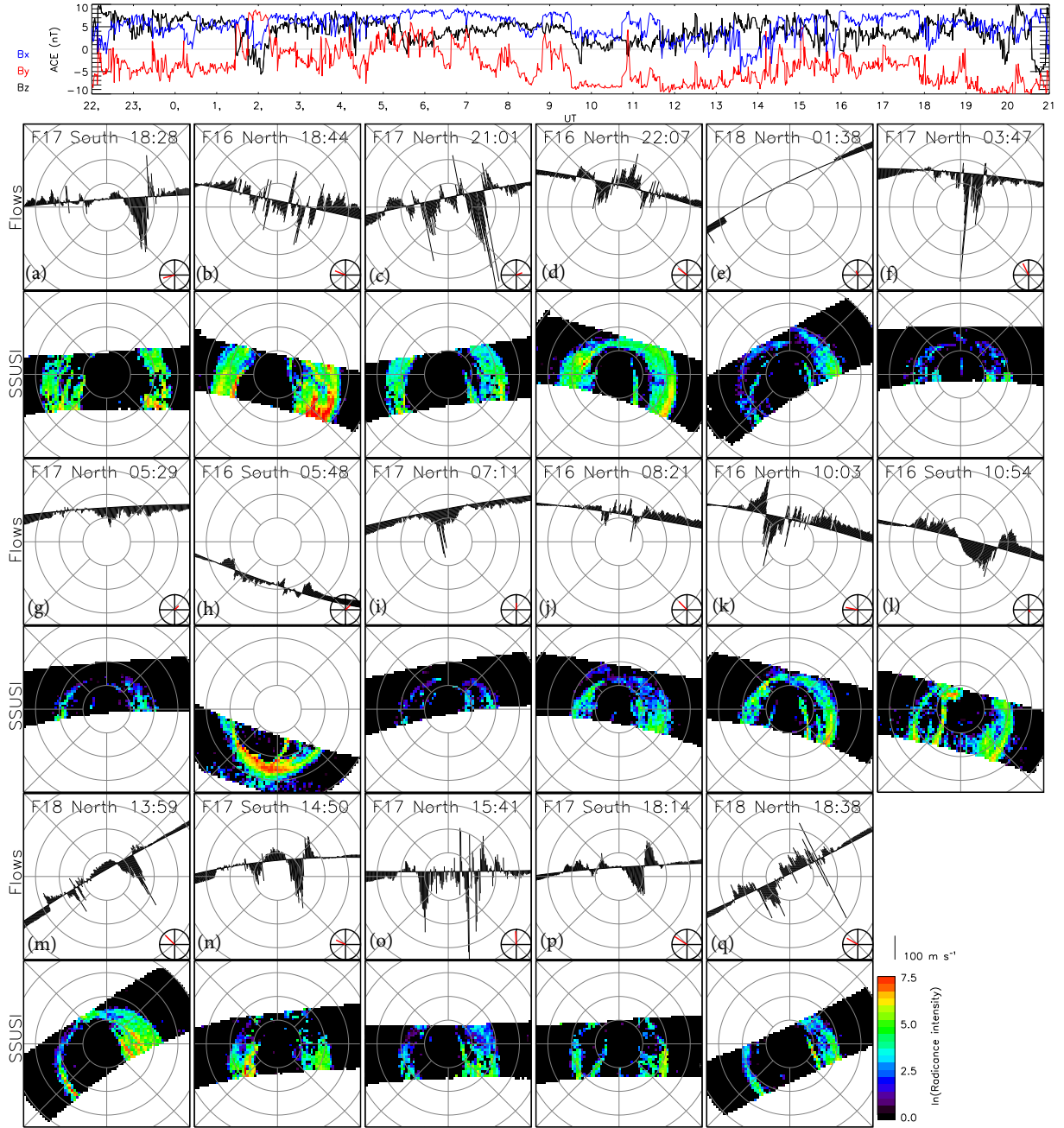


Figure 3: SSUSI images and IDM flows for event 1 with time increasing from left to right and top to bottom. The ACE data for the event is show in the top panel. The DMSP spacecraft ID, hemisphere and time are indicted in the top of each panel.

294 At 22:07 UT there were clear sunward flows associated with northward IMF and a potential
 295 HCA configuration began to develop but it is not clear in the south as the spacecraft passes
 296 were towards the nightside. The clock angle reduced around 21:40 UT and the magnitude of
 297 the B_y component decreased to less than -5 nT after around 22:10 UT and the B_z component

was northward with less variability. The ASC images were available from around 23 UT and a northward motion of the duskside of the polar cap was visible in these images particularly in the Resolute Bay camera. It is noted that the ASC were obscured by the presence of the Moon which moved from the south-east to the south of the ASC images throughout the event. The HCA pattern faded around 01:38 UT which was in a short dip between two periods of positive B_y (+5 nT) and slightly negative B_z . It can be seen in the Rankin Inlet images that the arc moved towards the southeast and in Resolute Bay it moved westward and Taloyoak did not see much.

The IMF returns northward around 2:15 UT and B_y became close to 0. The IMF then returned and stayed northward and B_y approximately 0 for approximately 5 hours with only a slight B_y dip to -5 nT around 4:30 UT. During this time the ASC did not see much. The DMSP flows were less clear with no sunward flows measured for these time in the northern hemisphere but some small sunward flows were seen in the southern hemisphere. Around 8:15 UT – 8:45 UT the IMF B_y dips to -5nT perhaps halting the HCA formation and causing the TPA to move back poleward.

During the second period of near-zero clock angle arcs were seen moving duskward in the ASC. A faint arc was visible in the Taloyoak data at around 9:09 UT and moved northward. It was not seen in the Resolute Bay north-south keogram as it does not cross the centre of the image. A fainter arc was seen by Resolute Bay at 9:11 UT that briefly moved northward before fading. The IMF B_y decreases again at 9:30 UT and the arc remained relatively stationary.

Around 9:20 UT and 10:05 UT an arc was visible in the field of view of Resolute Bay and then it also became visible in Taloyoak around 09:45 UT. This arc was moving south-eastward until 11:35 UT. A further arc was seen in the Resolute Bay image moving south-eastward around 10:20 UT leaving the field of view around 10:40 UT. This arc was faint and not clearly seen in the Taloyoak images. The IMF remained consistent until 14:30 UT and the arcs merged into the oval.

The HCA pattern re-appears around 14:50 UT (Figure 3n) when the IMF B_y increases to between 0 and -5nT. Sun-ward flows accompanied this HCA pattern and lasted until 18:33 UT. Around 18:00 UT the IMF B_y decreased again to -9nT then remained largely negative and the HCA pattern disappears.

In summary, a TPA formed in both hemispheres around four hours before the HCA event started. Changes in the IMF B_y and B_z component cause both the TPA and HCA to move throughout the event. Southward IMF causes equatorward motion where negative B_y caused

dawnward motion in the northern hemisphere which ended the event.

3.3 Dominated Positive B_y

We will present event 9 and discuss event 10 which are periods of HCA which end with the IMF being dominated by positive B_y .

Event 9 occurred on the 5th January 2016. The clock angle first approached zero around 11:55 UT and remained so for around 2 hours with slight deviations to positive B_y . The aurora was first seen in the Resolute Bay camera around 12:20 UT (Figure 1). The Rankin Inlet camera was obscured by a bright spot and therefore does not show anything. The Resolute Bay arc was then seen moving northward and left the field of view around 13:00 UT. Shortly after another arc was seen moving northward until the second arc disappeared northward of the field of view around 13:35 UT. Then there was a period where only faint arcs were seen on the southward edge of the field of view. A further third clear arc was seen around 13:55 UT; this arc quickly moved northward and a fourth arc followed it northward until 14:20 UT when it remained stationary. This stationary time occurred shortly after a quick southward turning of the IMF and increase in the magnitude of B_y . The arc was not as bright but continued moving northward after around 14:45 UT followed by other faint arcs. At 15:15 UT there were no more ASC images.

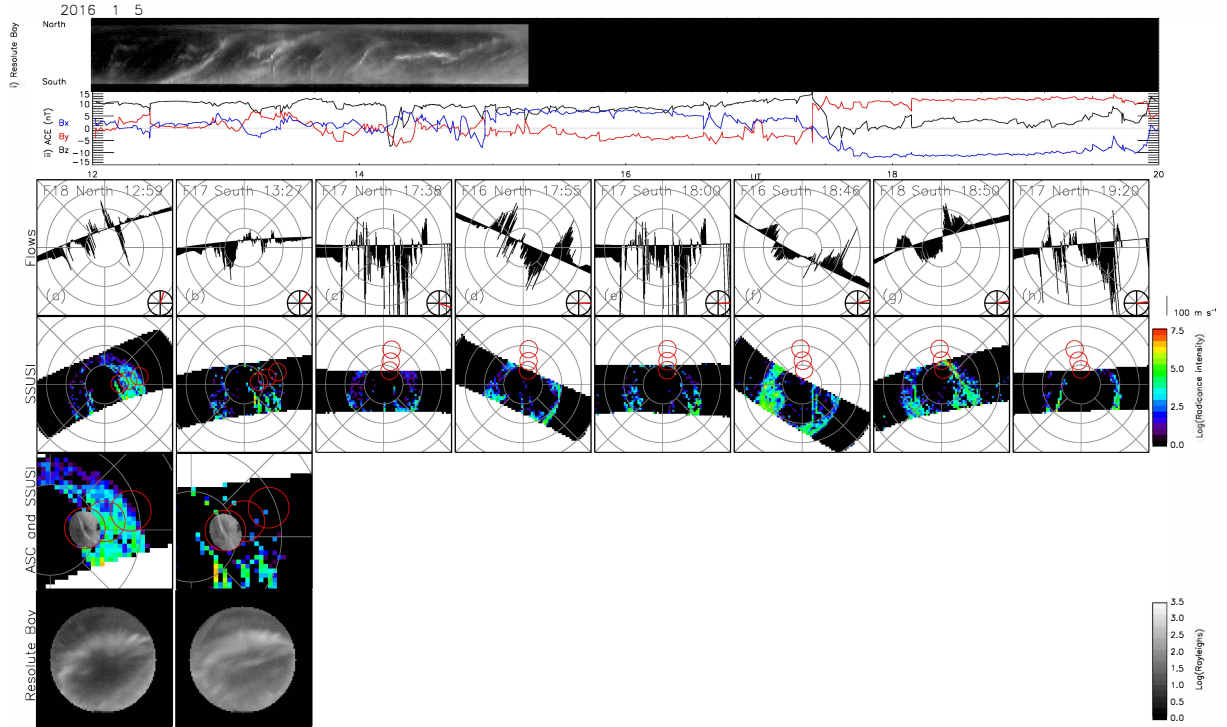


Figure 4: Event 9. Same format as Figure 1

Figure 4a shows the HCA pattern in the SSUSI image at 12:59 UT. The SSUSI images

also showed this multi arc structure showing the webs of the HCA in this event were filled with other arcs. The SSUSI image at 13:27 UT (Figure 4b) showed this multiple arc structure in the southern hemisphere. Some sunward flows over the centre of the polar cap were seen around the start of the event at 12:32 UT and these became more clearly northward IMF flows in successive SSUSI images, and were seen continuously until 17:38 UT, this was shortly after the IMF became B_y positive dominated. The IMF continued to be B_y dominated and the HCA pattern disappeared to be replaced with a single arc at dusk (dawn) in northern (southern) hemisphere (Figure 4g and h).

In summary, the HCA is seen to form after a period of small clock angle. Multiple arcs appear to be present in the ASC images progressing northward. The IMF became B_y positive dominated ending the event. It was seen in the SSUSI images that the HCA pattern was replaced with a single arc in each hemisphere. In the northern hemisphere this arc was at dusk whereas in the southern hemisphere it was at dawn.

Event 10 also began after a period of pure northward IMF with clear sunward flows seen over the polar cap and the HCA pattern became visible in the SSUSI images. The Resolute Bay ASC images also viewed the dawn side of the HCA and saw arcs moving northward. During a brief period of positive B_y the arc seen in the ASC became brighter and moved northward faster. The ASC data ends before the end of the event. The IMF went positive B_y dominated again and in the northern hemisphere the arcs moved duskward and in the southern hemisphere they are moved dawnward. The expected sunward flows are seen throughout the event particularly in the southern hemisphere.

4 Discussion

Here we have made use of high latitude all-sky cameras (ASC) along with data from DMSP/SSUSI and DMSP/IDM to observe the lifetimes of horse collar aurora (HCA) events. 11 events from the Bower et al. [2022] list of HCA events were found to have suitable data coverage by the Resolute Bay ASC. Additional ASC data from the Taloyoak and Rankin Inlet stations has also been used where available. Milan et al. [2020] suggested a formation model of HCAs based on dual-lobe reconnection (DLR) and their anticipated response to a change in IMF orientation. We have classified the 11 events based on the change in IMF orientation as the HCA pattern ends. 45% of the events were found to end with a southward turning of the interplanetary magnetic field (five events). The other six events were found to end under B_y dominated IMF with positive B_y occurring for two events and negative for the other four events.

Each of the events follows a formation similar to that suggested by Milan et al. [2020] with the HCA pattern emerging from the auroral oval after a period of northward IMF usually with a small clock angle (θ). Table 2 shows the average clock angle for the hour centered on the start time of the HCA event and r , where r is the measure of angular dispersion. An r of 0 is a uniform distribution and an r of 1 is concentrated in one direction [Mardia and Jupp, 2009]. The average magnitude of the clock angle is below 41° for all the events but this has not taken into account the uncertainty on the start time of the event. The uncertainty in the start time of the event is due to the start time being based on the DMSP/SSUSI images in order to confirm that the poleward motion of the arcs is occurring at both dusk and dawn. This therefore means that the start time is only as accurate as the frequency of the DMSP/SSUSI images. This formation is slightly different for event 1 which occurs when a TPA is already present in the polar cap this is discussed in more detail in section 4.1.

Event	1	2	3	4	5	6	7	8	9	10	11
θ ($^\circ$)	-34.00	-39.27	37.54	20.66	-27.21	-40.97	22.07	40.98	17.12	4.42	-1.19
r	0.02	0.98	0.67	0.73	0.79	0.93	0.99	0.80	0.95	0.90	0.97

Table 2: Table of average clock angle, θ , in the hour centred on the start time of the HCA events. r is the measure of angular disruption.

After the initial formation the particular motion of the HCA arcs in each of the events varies depending of the IMF conditions. As shown in event 3 around 9:38 UT (Figure 2) a short southward turning can halt the formation of the HCA and in this case even cause the arcs to move anti-sunward. This is similar to what happens when the IMF turns southward for a long period resulting in the end of the HCA event. Five events are identified to end due to a southward turning of the IMF. Of these events two end with only a slight negative IMF (greater than -2 nT) (events 6 and 8), the other three events are more variable. Event 4 ended with an average southward IMF of around -3 nT. Event 2 and 7 ended with an average southward IMF of around -4 nT. As predicted by the Milan et al. [2020] model the sunward flows stop as the HCA ends in each of these events. This is expected as following a southward turning reconnection will resume at the nose of the magnetopause and typical Dungey cycle anti-sunward flows will occur across the polar cap [Dungey, 1961, Cowley and Lockwood, 1992]. Three of the events end with the southward component of the IMF dominating (events 6, 4 and 2). These events follow the anticipated response of Milan et al. [2020], as shown in their Figure 7b, with the arcs moving equatorward and towards nightside. The nightside motion of the HCA pattern begins before the southward turning for event 4 however the IMF is close to zero and sunward flows

have also stopped therefore this motion is still in keeping with the expected motion.

Event 2 also has a small southward turning of the IMF before the end of the event however this is also seen to cause the arcs to retreat equatorward. For this event the southern hemisphere SSUSI image at 12:48 (Figure 1e) shows the retreat of the HCA arc back into the main auroral oval on both sides and the ASC at this time show that a similar retreat was happening in the northern hemisphere. This shows that the motion was happening in both hemispheres simultaneously.

Events 7 and 8 although ending with a southward turning of the IMF were also influenced by a B_y dominance. Event 8 initially was slightly B_y positive after the southward turning of the IMF around 12:21, the arcs continued to move anti-sunward and were pushed duskward by the asymmetrical flows associated with the B_y dominance. Then later around 13:23 the IMF became B_y negative dominated while also turning northward. The Resolute Bay camera observed the dawn arc which did not move much during this period and then the arc faded entirely when more southward dominated IMF occurred at 16:00.

Event 7 was dominated by a strong B_y positive component of the IMF but the motion was less clear due to the SSUSI images for the time period being very far towards the nightside and as such the arcs are not visible. The dusk arc also stopped being visible in the Resolute Bay camera around 06:19 but was seen to be move southward before this time. This is the expected motion of the arcs based on Milan et al. [2020] Figure 7c which shows that due to an asymmetrical addition of new open flux caused by the B_y dominance the HCA arcs are forced either duskward or dawnward based on the sign of B_y and the hemisphere viewed. For positive B_y in the northern hemisphere the motion is expected to be duskward as seen in event 7.

Of the six events that are found to end due to a B_y dominated IMF, four are dominated by negative B_y and two by positive B_y . The positive B_y events (9 and 10) both consist of multiple auroral structures making up the HCA pattern with the HCA arcs close to the pole and the web filled with the other arcs seen by the Resolute Bay camera. In both cases the Resolute Bay camera was viewing the dawnside arc and the data ended before the end of the HCA event. In the case of event 9 at 14:20 the aurora visible in the Resolute Bay camera remained stationary (Figure 4) around this time the IMF briefly turned southward and the negative B_y increased in magnitude. This brief southward turning is thought to halt DLR and therefore the HCA arc stopped progressing northward. It is likely that the arcs do not retreat equatorward as the southward turning is not long enough for substantial new open flux to be created on the dayside. Event 10 has a more variable IMF with short B_y positive dominated period throughout

the event. One such time is at 11:22 and it can be seen in the Resolute Bay camera that the arc at this time became brighter and progressed northward more rapidly.

In both events when the IMF became B_y positive dominated as expected the strong sunward flows in the centre of the polar cap stopped as lobe stirring began, due to single lobe reconnection occurring. The B_y dominance is stronger in event 9 then event 10. In event 9 the IMF changed around 17:25 and by the next SSUSI image the aurora was less intense (Figure 4c). The two main HCA arcs were still visible and by 17:55 (Figure 4d) the two arcs began to move duskward. This appeared to start with the dayside end of the arcs moving first. The next northern hemisphere SSUSI image was at 19:20 and only one arc remained at dusk. Alternatively in the southern hemisphere the HCA arcs were less defined (Figure 4f) but appeared to move leaving a dawnside arc (Figure 4g).

In event 10 the IMF became B_y positive dominated around 15:18 but had had a considerable B_y component before this time. The clear sunward flows ended around 16:15. More complicated flows occurred after and the webs of the HCA appeared to fade with the two arcs left visible. By 16:38 both arcs in the northern hemisphere had moved duskward. By 18:00 a single arc was seen at dusk. The southern hemisphere was less clear and there were gaps in the SSUSI data meaning that the next southern hemisphere SSUSI image that clearly showed the remainder of the arcs is the 18:49 image in which a single arc was visible at dawn.

In both of these cases the arcs moved in opposite directions in each hemisphere such that in the northern hemisphere they moved duskward and in the southern hemisphere they moved dawnward. This is in agreement with Milan et al. [2020] model Figure 7d where they predicted that under continued northward IMF with a positive B_y component single lobe reconnection would take place. In the case of positive B_y the dawn lobe cell is larger than the dusk. This single lobe reconnection in the northern hemisphere would then siphon open flux from the pre-existing polar cap and expand a new polar cap at dawn which in turn causes the closed flux of the HCA arcs to move together and move duskward. The motion would also be expected to be the opposite in the southern hemisphere as seen in events 9 and 10. Milan et al. [2020] also suggested that in the northern (southern) hemisphere a smaller new polar cap may extend at dusk (dawn). This can cause a protrusion of aurora at dusk (dawn). This appears to happen in the case of event 9 and is seen clearest in the northern hemisphere at 17:55 (Figure 4d). Milan et al. [2020] also noted that as this process is dependent on single lobe reconnection and as such the rate of motion of the arcs does not have to be the same in both hemispheres as the rate of single lobe reconnection can be different. In the case of the events studied here the

rates of motion in each hemisphere are unclear due to the nature of the instruments used, with DMSP/SSUSI providing images from each spacecraft of each hemisphere every 45 min and the ASC only being in the northern hemisphere.

The flow patterns seen by DMSP/IDM also support Milan et al. [2020] model. During both events there were clear sunward flows over the centre of the polar cap, then after the IMF became positive B_y dominated the flow pattern changed. In the northern hemisphere the flows shift so that a small sunward flow was seen towards dusk between the two lobe cells where the dawn cell was the larger of the two cells due to the positive B_y component on the IMF. This can be seen most clearly in event 9 at 17:55 (Figure 4d). The opposite is also expected in the southern hemisphere such that the dusk lobe cell was the largest and the small sunward flows were seen towards dawn. This can be seen in event 9 at 18:00 (Figure 4e). Due to gaps in the data and less clear flow structures it is not possible to determine if this is the case for event 10.

The other four events end with a negative B_y dominated IMF, these are events 1, 3, 5 and 11. As previously mentioned event 1 is a special case involving a TPA that is present before the HCA event and as such is discussed separately below. The data was not ideal for any of these three events with event 11 and event 3 having gaps in the SSUSI data and the ASC not covering the entire period and event 5 the HCA does not form very far into the polar cap before the IMF changes. In event 11 the HCA pattern takes a while to be seen clearly in the SSUSI data around 3 hours after the IMF became more northward. This could be due to the small magnitude of B_z (~ 2 nT) therefore the clock angle was effected more easily by changes in B_y . Once formed the HCA arcs progressed poleward with the web appearing to be filled with other aurora observed by Resolute Bay. There were some gaps in the SSUSI data but sunward flows were seen regularly. A negative B_y dominated between 13:11 and 13:30 which appeared to slow the motion of the dawnside arc seen by the Resolute Bay camera. This is possible under the Milan et al. [2020] model as the negative B_y could cause the dawnside arc to move slightly duskward before moving anti sunward if the negative B_y dominance continued. The duskside arc would also be expected to move dawnward but this was not visible as there was a gap in SSUSI observations at this time. Unfortunately the end of the event is less clear due to the data gaps in both SSUSI and the ASC along with the IMF being variable. The IMF was dominated by mainly B_y negative from 16:11 with a short positive dominance at 19:19-19:35. The SSUSI image at 18:59 showed a single arc on the duskside in the southern hemisphere and on the dawnside in the northern hemisphere at 19:39. The flows did not clearly show the flow pattern expected by Milan et al. [2020] as they are weak but the location of the arcs are in agreement

with the model. Events 3 and 5 also show the same motion of the arcs after the IMF became negative B_y dominated with the poleward arcs of the HCA moving towards dawn in the northern hemisphere and toward dusk in the southern hemisphere.

4.1 Event 1 Discussion

Event 1 is a special case as the HCA event occurs while there was a pre-existing TPA. The TPA formed around 4 hours before the start of the HCA. This TPA is consistent with the Milan et al. [2005] TPA formation model with the TPA being mirrored in each hemisphere about the Sun-Earth line. The TPA occurred at dawn in the northern hemisphere and at dusk in the southern hemisphere, this is consistent with the negative sign of the B_y component in the hours before the TPA event [Fear and Milan, 2012]. The IMF had a negative B_y component around -6 nT for at least an hour before the TPA began to protrude into the polar cap. After the formation of the TPA the IMF became variable with large B_y components. This variation lead to a complicated flow pattern until 22:07 UT when clear sunward flows were seen and a potential HCA configuration began to be visible in the SSUSI images. This formation maybe linked to the clock angle reducing around 21:40 UT, the B_y component increased to above than -5 nT after around 22:10 UT and the B_z component was northward with less variability. Figure 5a and 5b show a proposed flow pattern in the northern hemisphere adapted from Milan et al. [2020] Figure 3b and 3c to add the presence of a TPA formed under negative B_y . This potential HCA pattern and more stable IMF continued along with the sunward flow until 00:23 UT causing the TPA to move poleward.

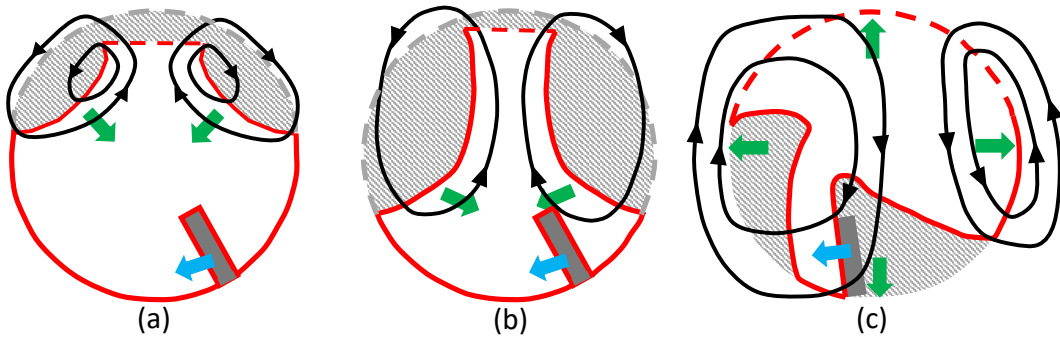


Figure 5: (a and b) HCA formation with pre-existing TPA. (c) Response to change in IMF southward turning and $B_y > 0$ in northern hemisphere. Light grey shaded area is the HCA, dark grey the TPA. Black arrow show the flow. Blue the motion of the TPA and green the expansion of the polar cap.

The IMF changed such that it is B_y positive between 01:27 UT and 01:36 UT and B_y negative between 01:36 UT and 01:45 UT. Along with this the B_z component became slightly

negative during the positive B_y . It is possible that this variation causes the flows to be like that of Milan et al. [2020] Figure 7(c) and adapted to include the TPA in Figure 5c. The aurora seen by Rankin Inlet and Resolute Bay matches the expected motion of the HCA with Rankin Inlet seeing the arc move south-east ward and Resolute Bay westward.

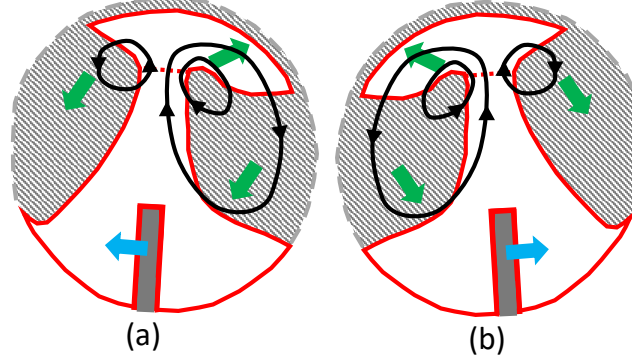


Figure 6: Motion of HCA and TPA with dominant B_y component in the northern hemisphere under northward IMF (a) $B_y > 0$ (b) $B_y < 0$. Light grey shaded area is the HCA, dark grey the TPA. Black arrow show the flow. Blue the motion of the TPA and green the the motion of boundaries of the polar cap.

Around 2:15 UT the IMF returned northward with a clock angle of around 3° for the next 5 hours with a r of 0.82 where r is the measure of angular disruption. An r of 0 is a uniform distribution and an r of 1 is concentrated in one direction [Mardia and Jupp, 2009]. The only deviation was a slight B_y dip to -5 nT around 4:30 UT. The flows would then be expected to return to those in Figure 5b thus causing the TPA to sit in the middle of the polar cap. During this time the ASC did not see much.

Between 04:57 UT and 07:11 UT the TPA was hard to distinguish from the HCA. This could be because when the B_y component was negative such that it had a higher magnitude and DLR stopped but with continued northward IMF the flows would be similar to Milan et al. [2020] Figure 7d with the larger flow cell being the dawn cell. Figure 6 shows the proposed motion of the HCA and TPA under B_y dominated northward IMF for Figure 6a $B_y > 0$ and Figure 6b $B_y < 0$. In the case of this event B_y was initially negative and went positive between approximately 4:45 UT and 6:15 UT. Therefore the TPA was moved across the polar cap downward and then duskward. Via these flows the TPA became indistinguishable from first the dawn arc of the TPA and then the dusk (Figure 3b), with the opposite true in the southern hemisphere. The DMSP/IDM flows were less clear with no sunward flows measured for these time in the northern hemisphere but some small sunward flows were seen in the southern hemisphere.

A dip in IMF B_y halted the formation of the HCA and caused the TPA to move back

552 poleward. When the IMF was again approximately zero the ASCs saw an arc moving from one
 553 camera to another. Figure 7 indicates this progression. The orange arrows in Figure 7 show
 554 the dawn arc of the HCA first moved northward in the Taloyoak image around 9:09 UT into
 555 the Resolute Bay camera when it moved duskward. It did not cross the centre of the image so
 556 was not seen in the north-south keogram. A fainter arc was seen by Resolute Bay at 9:11 UT,
 557 indicated by the blue arrow, briefly moved northward before fading.

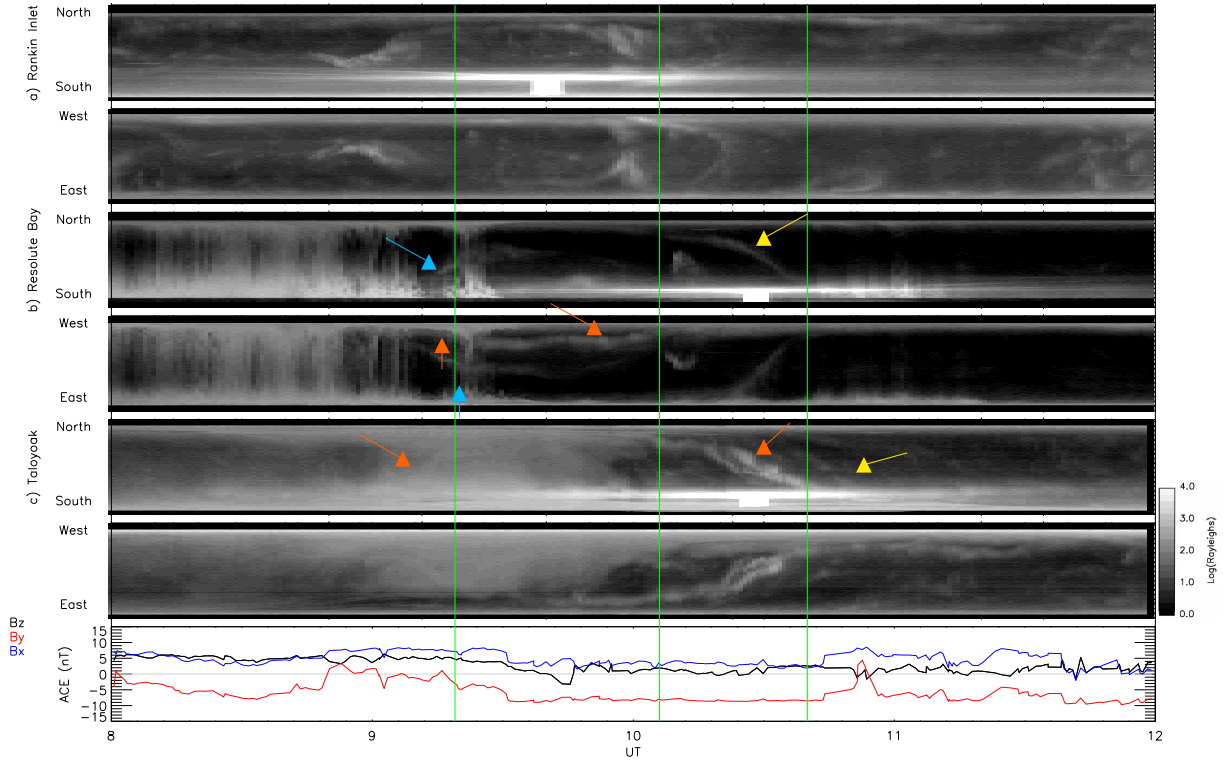


Figure 7: ASC keograms on 11th November 2014 8-12 UT with ACE data in bottom panel. The top two panels are the Rankin Inlet camera the next two are the Resolute Bay and the final two ASC panels are the Taloyoak camera.

558 Around 9:30 UT the B_y component changed to less than -9 nT and halted the formation of
 559 the HCA. The TPA was again visible in the centre of the polar cap. Again the flows could be
 560 expected to be like those in Figure 6b. At 10:03 UT (Figure 3k) the TPA then appeared as the
 561 dawn arc of the HCA, however there are two arcs visible on the dawnside, the most poleward is
 562 the TPA the other the HCA. The opposite is true in the southern hemisphere (Figure 3l).

563 The HCA dawn arc (orange arrows Figure 7) was visible in the field of view of Resolute Bay
 564 between around 9:20 UT and 10:05 UT. And it also became visible in Taloyoak around 09:45 UT
 565 and was clearly visible moving south and dawnward until 11:35 UT. A further arc (yellow arrows
 566 Figure 7) was seen in the Resolute Bay image to move south and dawnward around 10:20 UT
 567 and left the field of view around 10:40 UT. This arc is believed to be the TPA moving dawnward.

The arc was faint and not clearly seen in the Taloyoak images however there was aurora seen to move dawnward around 10:45 UT- 10:50 UT. This IMF configuration remained until around 14:30 UT and the TPA has merged with the oval and the HCA pattern has gone.

Then the IMF B_y increased to between 0 and -5nT and by 14:50 UT a HCA pattern was seen forming with sunward flows (Figure 3n). Sunward flows were seen consistently until 18:33 UT however a TPA dominated over the HCA pattern (Figure 3o). Around 18:00 UT the IMF B_y decreased again to -9nT we could expect the arcs in the northern hemisphere to be pushed dawnward (Figure 3q) as predicted by Figure 6b. B_y then remained largely negative -9nT and the HCA pattern disappeared and the TPA merged with the dawnside oval in the northern hemisphere.

5 Conclusion

We have studied 11 horse collar aurora (HCA) events with the use of DMSP/SSUSI and DMSP/IDM. In addition we have used three REGO all-sky cameras (ASC) located at Resolute Bay, Taloyoak and Rankin Inlet to improve the spatial and temporal resolution of the observations within the polar cap. The formation of these HCA occurs as expected under northward IMF during times when the clock angle is small. The evolution of the HCA is consistent with the Milan et al. [2020] model such that a southward turning of the IMF causes the HCA arcs to retreat equatorward toward the nightside. A B_y dominated southward IMF also causes the HCA arcs to move duskward if positive and dawnward if negative. A continued northward IMF with a large B_y component also causes the arcs to move in a dusk-dawn motion as predicted by Milan et al. [2020]. Under a B_y positive dominated northward IMF the HCA arcs move duskward in the northern hemisphere leaving the original dawnside arc of the HCA visible at dusk in the polar cap regions. The motion is opposite in the southern hemisphere. This motion is also reversed if the IMF is dominated by a negative B_y component such that in the northern hemisphere the arcs are left at dawn.

We also studied an event where a TPA occurs followed by a HCA. The TPA pre-exists the HCA by around 4 hours and is consistent with the Milan et al. [2005] TPA formation model, forming at dawn in the northern hemisphere. We then suggest how the TPA and HCA evolve in the context of the Milan et al. [2020] HCA formation model.

Acknowledgements

GEB is supported by a Science and Technology Facilities Council (STFC), UK, studentship.

SEM is supported by STFC grant no. ST/S000429/1. The work at the Birkeland Centre for Space Science is supported by the Research Council of Norway under contract 223252/F50. We acknowledge use of NASA/GSFC's Space Physics Data Facility's CDAWeb service, OMNI data and ACE data (at <http://cdaweb.gsfc.nasa.gov>). The DMSP/SSUSI file type EDR-AUR data were obtained from <http://ssusi.jhuapl.edu> (data version 0106, software version 7.0.0, calibration period version E0018). The Redline Auroral Geospace Observatory (REGO) is a joint Canada Foundation for Innovation and Canadian Space Agency project developed by the University of Calgary at (https://data.phys.ucalgary.ca/sort_by_project/GO-Canada/REGO/)

References

- G E Bower, S E Milan, L J Paxton, and B J Anderson. Occurance statistics of horse collar aurora. *Journal of Geophysical Research: Space Physics*, page e2022JA030385, 2022. doi: 10.1029/2022JA030385.
- University of Calgary. Redline geospace observatory (rego), 2022. URL <https://www.ucalgary.ca/aurora/projects/rego>. Last accessed 17th March 2022.
- S. W. H Cowley and M Lockwood. Excitation and decay of solar wind-driven flows in the magnetosphere-ionosphere system. In *Annales geophysicae*, volume 10,1-2, pages 103–115, 1992.
- J. W Dungey. Interplanetary magnetic field and the auroral zones. *Physical Review Letters*, 6(2):47, 1961. doi: 10.1103/PhysRevLett.6.47.
- R. C Fear and S. E Milan. The IMF dependence of the local time of transpolar arcs: Implications for formation mechanism. *Journal of Geophysical Research: Space Physics*, 117(A3), 2012. doi: 10.1029/2011JA017209.
- A Goudarzi, M Lester, S. E Milan, and H. U Frey. Multi-instrumentation observations of a transpolar arc in the northern hemisphere. In *Annales Geophysicae*, volume 26, pages 201–210. Copernicus GmbH, 2008. doi: 10.5194/angeo-26-201-2008.
- E W Hones, J D Craven, L A Frank, D S Evans, and P T Newell. The horse-collar aurora: A frequent pattern of the aurora in quiet times. *Geophysical research letters*, 16(1):37–40, 1989. doi: 10.1029/GL016i001p00037.
- K Hosokawa, A Kullen, S Milan, J Reidy, Y Zou, H U Frey, R Maggiolo, and R Fear. Aurora in the polar cap: A review. *Space Science Reviews*, 216(1):1–44, 2020. doi: 10.1007/s11214-020-0637-3.

- S. M Imber, S. E Milan, and B Hubert. The auroral and ionospheric flow signatures of dual lobe reconnection. *Annales Geophysicae*, 2006. doi: 10.5194/angeo-24-3115-2006.
- Jun Liang, E Donovan, B Jackel, E Spanswick, and M Gillies. On the 630 nm red-line pulsating aurora: Red-line emission geospace observatory observations and model simulations. *Journal of Geophysical Research: Space Physics*, 121(8):7988–8012, 2016. doi: 10.1002/2016JA022901.
- K Makita, C-I Meng, and S-I Akasofu. Transpolar auroras, their particle precipitation, and imf by component. *Journal of Geophysical Research: Space Physics*, 96(A8):14085–14095, 1991. doi: 10.1029/90JA02323.
- K V Mardia and P E Jupp. *Directional statistics*, volume 494. John Wiley & Sons, 2009.
- C-I Meng. Polar cap arcs and the plasma sheet. *Geophysical Research Letters*, 8(3):273–276, 1981. doi: 10.1029/GL008i003p00273.
- S E Milan, B Hubert, and A Grocott. Formation and motion of a transpolar arc in response to dayside and nightside reconnection. *Journal of Geophysical Research: Space Physics*, 110(A1), 2005. doi: 10.1029/2004JA010835.
- S E Milan, J A Carter, G E Bower, S M Imber, L J Paxton, B J Anderson, M R Hairston, and B Hubert. Dual-lobe reconnection and horse-collar auroras. *Journal of Geophysical Research: Space Physics*, 125(10):e2020JA028567, 2020. doi: 10.1029/2020JA028567.
- JS Murphree, CD Anger, and LL Cogger. The instantaneous relationship between polar cap and oval auroras at times of northward interplanetary magnetic field. *Canadian Journal of Physics*, 60(3):349–356, 1982. doi: 10.1139/p82-047.
- L J Paxton, C-I Meng, G H Fountain, B S Ogorzalek, E H Darlington, S A Gary, J O Goldsten, David Y Kusnierkiewicz, Susan C Lee, Lloyd A Linstrom, et al. Special sensor ultraviolet spectrographic imager: An instrument description. In *Instrumentation for planetary and terrestrial atmospheric remote sensing*, volume 1745, pages 2–15. International Society for Optics and Photonics, 1992. doi: 10.1117/12.60595.
- L J Paxton, C-I Meng, G H Fountain, B S Ogorzalek, E H Darlington, S A Gary, J O Goldsten, D Y Kusnierkiewicz, S C Lee, L A Linstrom, et al. Ssusi: Horizon-to-horizon and limb-viewing spectrographic imager for remote sensing of environmental parameters. In *Ultraviolet technology IV*, volume 1764, pages 161–176. International Society for Optics and Photonics, 1993. doi: 10.1117/12.140846.

- 660 L J Paxton, R K Schaefer, Y Zhang, and H Kil. Far ultraviolet instrument technology. *Journal*
661 *of Geophysical Research: Space Physics*, 122(2):2706–2733, 2017. doi: 10.1002/2016JA023578.
- 662 Frederick J Rich and Marc Hairston. Large-scale convection patterns observed by dmsp. *Journal*
663 *of Geophysical Research: Space Physics*, 99(A3):3827–3844, 1994. doi: 10.1029/93JA03296.
- 664 T Tanaka, T Obara, M Watanabe, S Fujita, Y Ebihara, and R Kataoka. Formation of the
665 sun-aligned arc region and the void (polar slot) under the null-separator structure. *Journal of*
666 *Geophysical Research: Space Physics*, 122(4):4102–4116, 2017. doi: 10.1002/2016JA023584.
- 667 L Zhu, R. W Schunk, and J. J. Sojka. Polar cap arcs: A review. *Journal of Atmospheric and*
668 *Solar-Terrestrial Physics*, 59(10):1087–1126, 1997. doi: 10.1016/S1364-6826(96)00113-7.